Chip-Based Cardiac Arrhythmia Modeling: Drug Response Investigation and Structural Deformities Impact Assessment

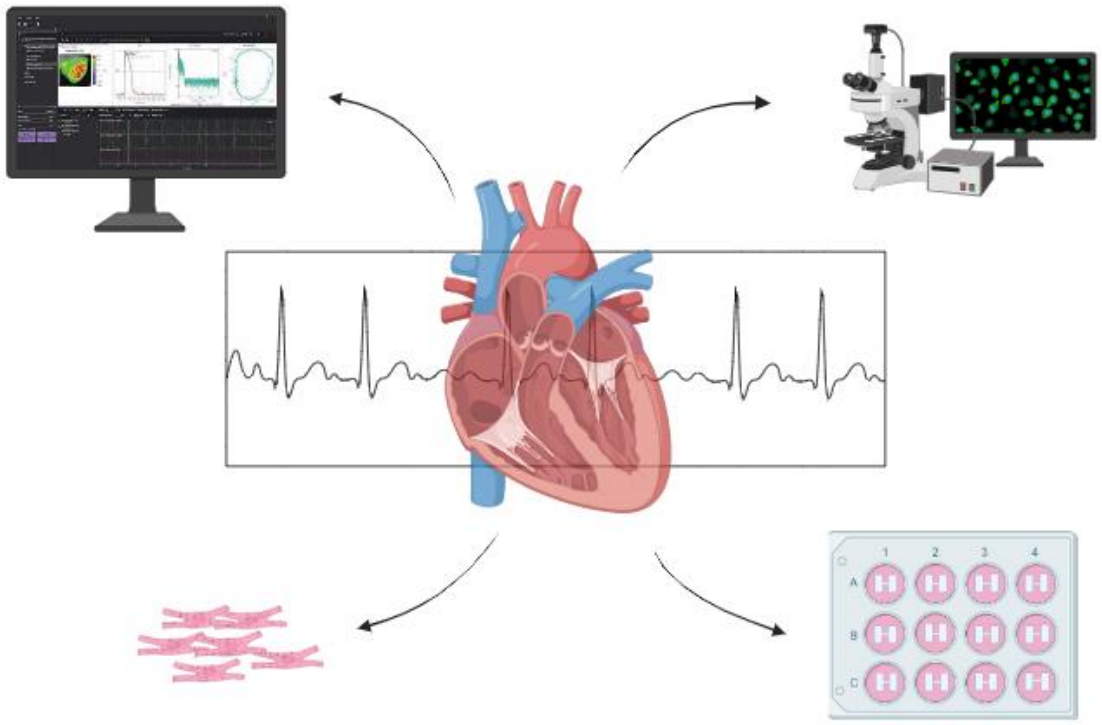

MASTER THESIS

SWATHIKA R.S

s2847183

Faculty of Science & Technology

MSc Biomedical Engineering

Applied Stem Cell Technologies (AST)

University of Twente

Enschede, The Netherlands

Examination committee:

Prof. Dr. P.C.J.J. Passier (Robert)

Dr. V. Schwach

Prof. Dr. Jeroen Leijten

M. Dannenberg MSc

UNIVERSITY OF TWENTE. | TECHMED CENTRE

ACKNOWLEDGEMENTS

Over the past 10 months, I engaged in my master's graduation assignment within the Applied Stem Cell Technologies (AST) research group at the University of Twente. This experience has been immensely enriching, particularly through my involvement in the captivating project centered on designing a heart-on-chip model for the study of cardiac arrhythmia.

I extend my heartfelt gratitude to Dr. Verena Schwach and Maureen Dannenberg for their invaluable supervision throughout this project. Your guidance, both within and outside the lab, has been instrumental in my growth as a scientific researcher. The constructive suggestions and feedback you provided significantly contributed to the quality of my thesis, and I am proud of the outcome.

I am grateful to Prof. Dr. Robert Passier for offering me the opportunity to undertake my master's assignment at AST and for chairing my examination committee. I also express my appreciation to Prof. Dr. Jeroen Leijten for serving as an external member of my examination committee.

A special thanks to Mariel for her dedication to conducting experiments and engaging in insightful discussions throughout my assignment and a special recognition goes to José Rivera Arbeláez for his role in designing and fabricating the arrhythmia culture plate and helping with Imaging.

To my colleagues at the AST group, thank you for your unwavering willingness to assist me whenever needed. Finally, a shout-out to the fantastic individuals at the black table – the students with whom I had great discussions and enjoyable coffee breaks. Your camaraderie added a wonderful dimension to my time at AST. Thank you all for making this journey memorable.

I would like to express my deepest appreciation to my family, friends and loved ones for their unwavering support, love, and belief in me.

I am thankful to all those who have played a part in shaping this research study and making it a meaningful and rewarding experience.

TABLE OF CONTENT

ABSTRACT

Ischemic heart disease (IHD) and stroke stand as the leading causes of death and disability on a global scale. Cardiovascular diseases (CVDs) contribute *significantly* to disability, with many cases attributed to the consumption of alcohol, tobacco, nicotine, and caffeine. Cardiac arrhythmia, affecting over 12 million people worldwide, poses a substantial burden on healthcare systems. Despite this, the development of anti-arrhythmic drugs has seen limited progress. The prevalence of arrhythmia is estimated to affect 1% to 1.5% of the population, with challenges in estimating occurrence rates due to some individuals experiencing no symptoms. A comprehensive total of 464 pharmaceutical products were withdrawn from the market due to safety concerns. The primary reason includes cardiovascular toxicity. It is imperative to conduct a comprehensive examination of the fundamental mechanisms causing cardiovascular toxicity to avert the prolonged usage of potentially hazardous drugs, especially given that specific cardiovascular medications persisted on the market for extended durations. This emphasizes the need for the advancement of a more reliable human-based *in vitro* model that can be employed to investigate the mechanisms of arrhythmia. Recent advancements in *in vitro* stem cell tech and in silico modeling offer more models for heart failure and arrhythmia evaluation, addressing these challenges. This study addresses this need by designing an arrhythmia shape, creating a vulnerable substrate for cardiac arrhythmia by mimicking the source-to-sink mismatch in cardiac tissue. Arrhythmia-like events were induced by subjecting cardiac tissues to Epinephrine and electrical pacing, and subsequent experimentation revealed that Amiodarone successfully counteracted the effects of Epinephrine on our cardiac tissue in the PDMS shape. Limited experiments on cardiac tissues cultured in the arrhythmia shapes showed minimal counteracting effects of Amiodarone. Despite these constraints, this study marks the next step in designing a heart-on-chip model for the study of cardiac arrhythmias. Looking ahead, there is potential to further develop this heart-on-chip model into a comprehensive, multidisciplinary platform for the risk assessment of cardiac arrhythmias.

1. Introduction

1.1.Cardiac diseases and occurrence

Cardiovascular diseases (CVDs) and stroke are the primary causes of death and disability worldwide. Most cardiovascular diseases result from the intake of alcohol, nicotine, and caffeine [1]. Fighting cardiovascular illnesses and complications caused by conditions such as arrhythmia is still an unmet need. Even though there hasn't been much focus on understanding the mechanism of cardiac arrhythmia, massive efforts have been made to develop therapeutic solutions to cardiac complications and diseases[2]. Irregular metabolism and energy imbalance can lead to metabolic consequences. The risk of cardiac arrhythmia is higher in people with diabetes, obesity that may lead to heart attack/ stroke [3],[4]. Globally, over 12 million people get affected by cardiac arrhythmia. An estimate of 1% to 1.5% of population is affected by arrhythmia but some asymptomatic people making it difficult to estimate the occurrence rate of arrhythmia [5]. The morbidity and mortality of millions of patients are still greatly impacted by cardiac arrhythmia, despite tremendous advancements in its detection, treatment and management. This is partially due to unmet knowledge gaps in the cardiac pathophysiology, screening, and therapeutic approaches of arrhythmia, such as rate/rhythm control and stroke prevention [6]. Reproducing the patterns of action potential (AP) propagation in the human heart during sinus rhythm and arrhythmia is crucial to produce useful models for researching the mechanisms underlying atrial arrhythmias. In addition to simulating high-frequency focused activity and anatomical and functional reentry, these capabilities allow researchers to analyze the function of certain disease pathways or arrhythmia mechanisms [7]. Automaticity, trigger activity, and reentry are three basic mechanisms on which cardiac arrhythmia relay on. If any of the mechanisms has abnormal activity or delay in their activity that might lead to arrhythmia [8]. There are different types of arrhythmias, each type with its own symptoms and can occur in any part of the heart but heart rate being fast or slow or irregular is the most common symptom of all types of arrhythmias [9]. The most common symptoms of arrhythmia are palpitations, chest discomfort, dizziness, and shortness of breath and in worst case it leads to death. But arrhythmia can also occur without symptoms [10]. From 1950 to 2017, a comprehensive total of 464 pharmaceutical products were withdrawn from the market due to safety concerns. The primary reason for withdrawal was hepatotoxicity, followed by neurotoxicity and cardiovascular toxicity. A thorough investigation into the underlying mechanisms of cardiovascular toxicity is crucial to prevent the prolonged use of potentially risky drugs, particularly considering that certain cardiovascular medications remained on the market for extended periods[11],[12].

1.2. Healthy heart vs Arrhythmic heart

The heart is divided into four chambers which are atria on the top and ventricles below. Four chambers are divided by one-way valves that open and close with each pulse. Normal sinus rhythm (NSR) is the name for a healthy heartbeat. Arrhythmia is a condition when heart rhythm/heart rate are irregular[13].

The heart contracts because of an electrical signal which begins in the sinoatrial node and through the atria it reaches the atrioventricular node. The ventricles then go through one cycle of contraction once activation has spread across them. In the Figure 1, it is shown that this coordination of electrical signals is disrupted in arrhythmic heart (right side) when compared to the normal heart (left side) [14]. The reentry phenomenon, in which the electric stimulation cycles around a core of unexcitable tissue, is often the underlying cause of arrhythmia [15]. Understanding the underlying mechanism of cardiac arrhythmia at the cellular level can be helpful to clinically manage and treat arrhythmia of all types [16]. Recently,

researchers have focused on replicating the organ level physiology in a chip with the help of the bioengineering technologies which would greatly improve the disease modeling and help with high throughput drug screening [17]. With suitable cell sources, mechanical designing the heart on a chip can be used for *in vitro* modelling and to gain insights of the mechanisms which will pave a way for understanding cardiovascular diseases and associated drug screening processes [18].

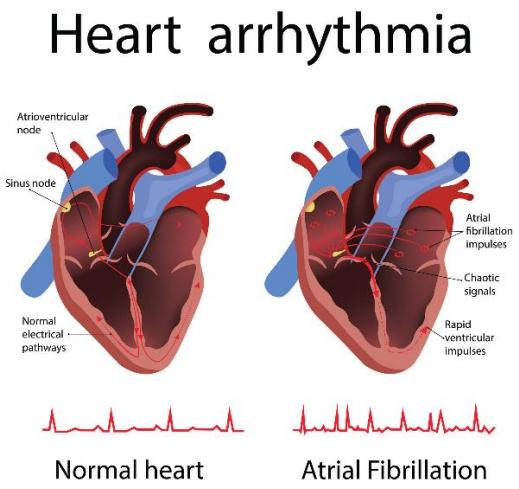

Figure 1: The coordination of electrical signals in normal heart vs arrhythmic heart [14]

1.3.In vitro models and Heart-on-a-chip

The discipline of cardiac tissue engineering has been quickly producing more precise functional 3D cardiac microtissues from human cell sources because of recent advancements in stem cell biology, materials science, and bioengineering. The main goal of the *in vitro* 3D models is mimicking the function in disease and achieving high-throughput results of drug screening. These created tissues allow for the screening of cardiotoxic medicines, disease modeling and they can act as new drug development platforms [19],[20]. Traditionally, arrhythmia research relied on affected individuals or animal models, but limitations like interspecies variation and ethical concerns prompted a shift. Recent advancements in *in vitro* induced pluripotent stem cell technology and in silico modeling have diversified models for heart failure and arrhythmia assessment[12]. Earlier scientists relied on 2D monolayer heart models to study the mechanism of the disease and to evaluate drug reactions. It is also known that animal models are used for drug testing procedures. Using 3D tissue models with stem cells would be more ethical and reliable as the animal models do not represent human physiology [21]. This underscores the need for the advancement of a more reliable human-based *in vitro* model that can be employed to investigate the mechanisms of arrhythmia. Recently, cardiomyocytes and other types of heart cells can be employed in the growing area of Heart-On-a-Chip (HOC) technology to create functioning cardiac microtissues which replicate many characteristics of the human heart. HOC models are set to play a significant role in the drug development process and show considerable potential as disease modeling platforms. Diseased HOCs are highly tunable and can be produced using a variety of methods, including using cells with known genetic backgrounds (patient-derived cells), adding small molecules, altering the cell's environment, and changing the cell ratio/composition of microtissues, among others. This is made possible by advances in

the biology of human pluripotent stem cell-derived cardiomyocytes and microfabrication technology [22]. Invitro animal models have been used as research models for studying cardiac mechanisms and its disease modeling for over a decade. But with its limitations of mimicking the human pathophysiology and inability to alter the mechanical and structural properties results in complicated cardiovascular research for comparing electrophysiology properties of cardiac cells since the rodents have short span of repolarization time than humans [23],[24]. 3D cardiac tissue models resolve these limitations by allowing researchers to mimic the human heart characteristics in a chip-based model using human induced Pluripotent Stem Cells (hiPSC) derived cardiomyocytes.

1.4.Cardiomyocytes

This project utilizes Pluripotent Stem Cell-Cardiomyocytes (hiPSC-CMs), specifically sourced from the WTC cell line. These hiPSC-CMs are known for their capability to mimic human heart physiology, enabling to observe their reaction to different drugs. This approach holds promise for developing personalized medicine tailored to individual responses. In preparation for experiments, the differentiated cardiomyocytes are retrieved with appropriate safety measures and thawing is accomplished using a warm water bath, rendering the cells ready for use.

1.5.Arrhythmia-on- a- chip

This study aims to replicate an arrhythmia disease model using a chip-based design and assess the response of anti-arrhythmic drugs on this model. Literature proves that structural abnormalities in the heart can contribute to a higher incidence of arrhythmia, potentially leading to fatal outcomes[18]. The chip is designed from computer simulations and the design is adapted from existing literature to create a scenario where the electrical signal passing through a narrow channel may unevenly spread on the other side, potentially causing irregular contractions, and initiating arrhythmia. In the Figure 2E, an activation map of the neonatal rat ventricular myocytes (NRVM) monolayer on the heterogenous structure with a 1-mm wide isthmus is displayed [18]. Before inducing arrhythmia, a heart model must be generated, and the substrate for cardiac arrhythmia in this study is adapted from the source-to-sink mismatch, as depicted in Figures 2A-2D. Activation occurs when the source volume is larger (2A) or equal (2B) to the sink volume, ensuring sufficient electrical current for myocardial cell activation in the distal direction. Conversely, when the source volume is smaller than the sink volume, the activation wavefront may either slow (2C) or block (2D) denoted by the double black line, due to reduced electric current available for activating myocardial cells in the distal direction[25]. Invitro animal models have been used as research models for studying cardiac mechanisms and its disease modeling for over a decade. But with its limitations of mimicking the human pathophysiology and inability to alter the mechanical and structural properties results in complicated cardiovascular research for comparing electrophysiology properties of cardiac cells since the rodents have short span of repolarization time than humans [23], [24]. 3D cardiac tissue models resolve these limitations by allowing researchers to mimic the human heart characteristics in a chip-based model using hiPSC derived cardiomyocytes.

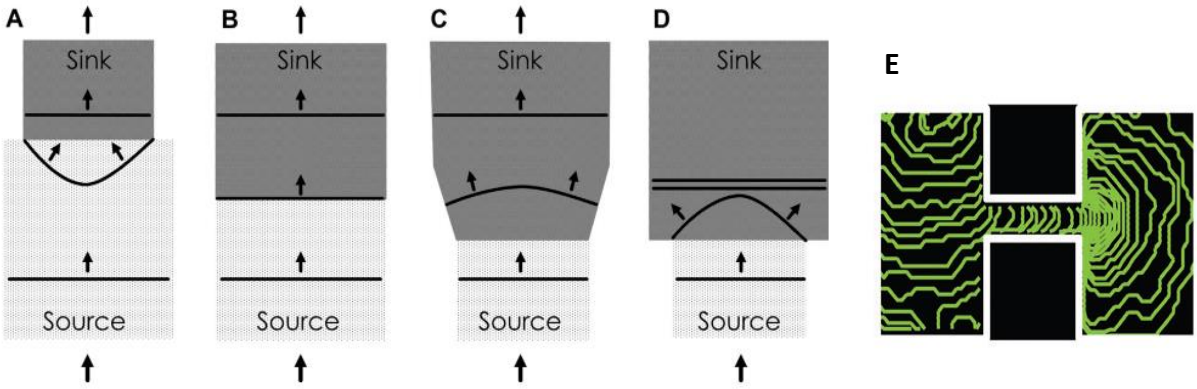

Figure 2: Discrepancy between source and sink resulting in reentry*. (A-D) Illustration of source-to-sink mismatch and its impact on electrical conduction at the isthmus boundary*[25]*. (E) Activation map displaying 5 ms isochrone lines for a patterned (NRVM) monolayer with a 1-mm-wide isthmus, paced at 6 Hz* [18], [25].

1.6. Anti-arrhythmic drugs on the arrhythmic shape

The goal of this arrhythmic model is to test anti-arrhythmic drugs and observe the effect on arrhythmia induced hiPSC-CMs in response to the drugs. Arrhythmic events are triggered in CMs using alpha- and beta-adrenergic agonists like epinephrine which increases the heart rate by modulating the ion channels. The channels that contribute to pacemaker activity and are impacted by -adrenergic stimulation are those that are most likely to be implicated. Adrenergic agonists also increase the intracellular Ca^{2+} concentration in atrial, ventricular and atrioventricular pacemaker cells which will result in the increased heart rate [26]. Epinephrine, caffeine, and alcohol are adrenergic agonists that used to increase the beating of cardiomyocytes in the cardiac tissues. Once increased pace of beating is observed, anti-arrhythmic drugs are tested on the cardiomyocytes in different concentration at different timepoints and the results are analyzed using statistical analysis to compare the effect of these drugs on the cardiomyocytes. There are four classes of anti-arrhythmic drugs such as class I, sodium-channel blockers; class II, beta-blockers; class III, potassium-channel blockers; class IV, calcium-channel blockers in which Amiodarone is a class III anti-arrhythmic drug which can block multiple channels including potassium and sodium channels. Amiodarone blocks the potassium channels that causes repolarization and increase in beating rate in the cardiac tissues [27]. After optimizing the arrhythmia model using these experiments, the cardiomyocytes are introduced to electrical pacing which would increase the beating of the cells according to the corresponding voltage and different frequencies (Hz) and anti-arrhythmic drugs are tested on the optimized arrhythmic model. In this study, we optimized the 1) chip material and its culture conditions, 2) Xanthan gum concentration, 3) Fluorescent staining method and analyzed the effect of anti-arrhythmic drugs on our cardiac tissue.

2. Materials and Methods

2.1.PDMS and PMMA fabrication

Two thermoplastic materials commonly utilized for chip models are PDMS and PMMA, recognized for their cell attachment and growth properties. In this project, both PDMS and PMMA chips were produced. PDMS chips were created by thoroughly mixing the PDMS mold and curing agent at a 10:1 ratio. The

mixture was then degassed in a desiccator until all bubbles were eliminated. The degassed mixture was poured into a cast with a negative resist of dumbbell shapes, secured with clamps, and placed in a degassing apparatus until all bubbles disappeared. Following degassing, the cast with the mold was cured in an oven for 24 hours. The hardened mold was carefully separated from the cast, and individual chips were obtained by cutting the mold. To ensure cell fixation in the desired shape, chips and 15 mm glass slides, to which the chips were attached, underwent plasma treatment using a plasma cleaner machine with a loaded PDMS recipe. The chip was immediately affixed to the glass slide, and the entire assembly was placed inside a 12-well plate, resulting in a ready-to-use PDMS chip which is shown in the Figure 3B, and the dimension of the shape is illustrated in the Figure 3C.

In Figure 3A, PMMA shapes were designed in a 12-well plate configuration, with each well featuring a dumbbell shape for cell seeding and the PMMA plate incorporates extruded shapes with PCR tape covering the bottom of the plate, facilitating cell culture.

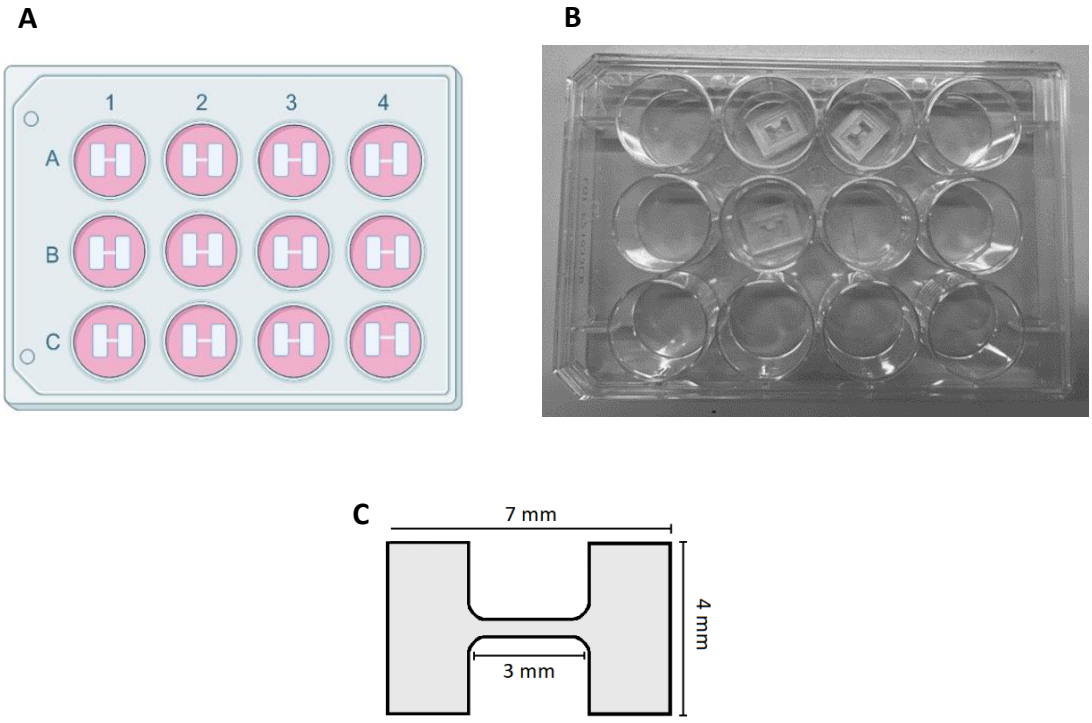

Figure 3: Design of the PMMA and PDMS shapes*. (A) Representation of the PMMA plate with arrhythmic shapes extruded. (B) 12-well plate with PDMS shapes (C) A detailed depiction of the dimensions of the PDMS shape.*

2.2.Cell seeding

Both the PDMS and PMMA plates underwent surface coating with a mixture of Matrigel (1:100, Corning) and Geltrex (1:100, Gibco) in DMEM/F12 (DMEMF12 1:1 (1x) + GlutaMAX-I, Gibco). To achieve optimal cell attachment, 20 µl of this solution is applied to the PMMA shape and 25 µl is applied to the PDMS plate, followed by a 1-hour incubation at 37°C. After this incubation period, the coating solution is removed, and DMEM/F12 medium containing 10% Fetal Bovine Serum (FBS, Gibco) and 2 µl of primocin for antibiotic protection is added. This FBS coating is allowed to incubate for approximately 2.5 hours before seeding the shapes with cardiomyocytes (CMs). Around 3.5 million cells are utilized for seeding,

with 500K cells/shape for PMMA and 600K cells/shape for PDMS. Upon thawing the cells, 4 ml of DMEM/F12 medium is added to the tube, and the cells are centrifuged to form a cell pellet. Post-centrifugation, 1 ml of high glucose (1:30) cardiomyocyte maturation TDI medium (CM medium) is added to the cell pellet to create a cell suspension. The concentrations of the growth factors 3,3',5'-Triiodo-L-thyronine (T), Dexamethasone (D), and long R3 IGF-I Human (I) are 100 nM, 1 µM and 100 ng/ml respectively. This suspension is then transferred to a polystyrene tube with a cell strainer cap for filtration. An additional 1 ml of CM medium is added to the filter tube for dilution, and the cell density is calculated using the hemocytometer technique. Following centrifugation and removal of the supernatant, a working solution of CM medium with collagen I (2 µg/mL, OptiCol Human Collagen Type I, Cellgs) and collagen III (3 µg/mL, OptiCol Collagen Type III, Cellgs) is prepared. The appropriate amount of this medium is added to the cell pellet, and the cell suspension is resuspended. Subsequently, 20 µl of this cell suspension is added to each shape of the PMMA plate and 25 µl to the PDMS shape. After a 1.5-hour incubation, 400 µl of CM medium is gently added to each shape without disturbing the cells. To ensure proper shape formation and attachment of the cells to the bottom, a Xanthan gum powder solution (1.5% w/v, Sigma-Aldrich) in CM medium is prepared on a roller bank overnight. The next day, 175 µl of this mixture is added to the top of each shape. Each well is then filled to the top with CM medium on the third day, and the medium is refreshed every two days. Once the cells exhibit efficient beating, imaging can be performed between day 9 and day 12 using NIKON Eclipse Ti2 microscope.

2.3.Calcium staining

Fluo-8 dye AM is a green, fluorescent calcium dye used for imaging calcium transient signals when the cardiomyocytes start contracting. Binding of Ca2+ with the dye makes the fluorescent intensity increase and it can be imaged. Usually between the 9^{th} and 12^{th} day, the cells are dyed with a working solution of 12 µM Fluo-8 AM in HBSS (Hank's balanced salt solution, Gibco). 1:16 Pluronic F-127 is added to increase the aqueous solubility of the dye. 100 µl of this working solution is added to shapes and are incubated for 1 hr. at 37°C. After 1hr, the cells are washed with HBSS, and fresh CM medium was added to the shapes. The cells were imaged for Ca2+ transient signals as they beat, and the image data were analyzed.

2.4.Testing anti-arrhythmic drugs on the cardiac tissue

In this study, the class III anti-arrhythmic drug Amiodarone is utilized to assess its impact on cardiac tissue. The cardiomyocytes are initially stained with a calcium fluorescent dye, as detailed in the preceding section, and baseline data is obtained through tissue imaging. Subsequently, the adrenergic stimulant Epinephrine is introduced at a concentration of 0.1 µM to enhance the contraction rate of cardiomyocytes. The cardiac tissue is incubated for 5 minutes and imaged for analysis to check if the beating of the cardiac tissue has increased. Following the removal of Epinephrine, the first concentration (0.1 µM) of Amiodarone is added, and the tissue is imaged for either 5 secs or 10 secs based on the beating rate. Subsequently, the solution is removed, and the second concentration (1 µM) of Amiodarone is introduced, followed by a 5-minute incubation period. The tissue is then imaged for analysis. Output data are stored in. nd2 files, which were analyzed using ImageJ software to generate graphs for comparing contraction rates at different time points and BV bench software to create activation time maps.

3. Result and Discussion

3.1.Enhanced Tissue Integrity in OoC Fabricated from PDMS Compared to PMMA

The experiment commenced by optimizing the ideal material and conditions to maintain the shape in culture. To robustly generate cardiac tissue in dumbbell shape, we first optimized the culture conditions. The incubation time for FBS coating was optimized from 1 hour to 2.5 hours in PDMS shapes. Notably, after cell seeding, the CM medium was introduced 1 hour after incubation in PMMA, while in PDMS, it was added after 1.5 hours, resulting in more consistent cardiac tissue formation with PDMS shapes than with PMMA. The overall optimized culture conditions for PMMA and PDMS is depicted in the Figure 4A. After several experiments, it was evident that the culturing of cells was uniform, and the cells had better attachment in PDMS than in PMMA shapes. The cells also had good syncytium in PDMS shapes. The cardiac tissue formed a nice dumbbell shape connected through the channel and the cells contracted at a uniform pace around D-7 as shown in the Figure 4C. The effectiveness of electrical pacing relies on the cells exhibiting strong attachment and forming a complete dumbbell shape. The clear observation of electrical signal propagation is possible only when there is a complete formation of the cardiac tissue. On the contrary, Figure 4B shows that there was no consistent shape formation without breakage in the channel and the cells only formed clusters in the PMMA chip. Despite numerous attempts with PMMA, it failed to uphold a satisfactory cell structure. As a result, it is concluded that PDMS shapes can be used for further experiments. This PMMA chip offers superior design and chip stability compared to the PDMS chip. The differences observed between the PDMS and PMMA chips are mentioned in the Table 1.

Although PDMS allowed for the formation of a complete cardiac tissue, issues arose during imaging as the PDMS chips were not affixed to the wells plate, complicating the analysis of data obtained through fluorescent imaging. To address this challenge, a UV-radiated 12-well plate with holes in the center of each well was utilized, ensuring the PDMS shapes remained fixed to the bottom of the wells plate. The PDMS shapes, combined with 18 mm glass slides, were secured using MOLYKOTE® DC High-Vacuum Grease. The enhanced shape demonstrates improved cell attachment and the successful formation of the desired structure as shown in the Figure 4D. Additionally, this resolution addresses the imaging challenges associated with PDMS shapes, as outlined in the table above. This optimization provides an ideal basis for advancing the research to the next stages.

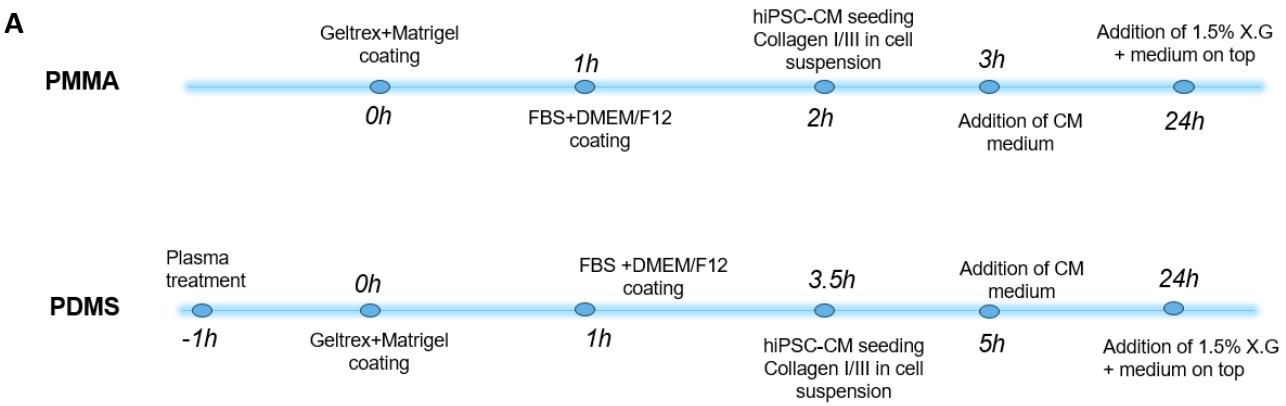

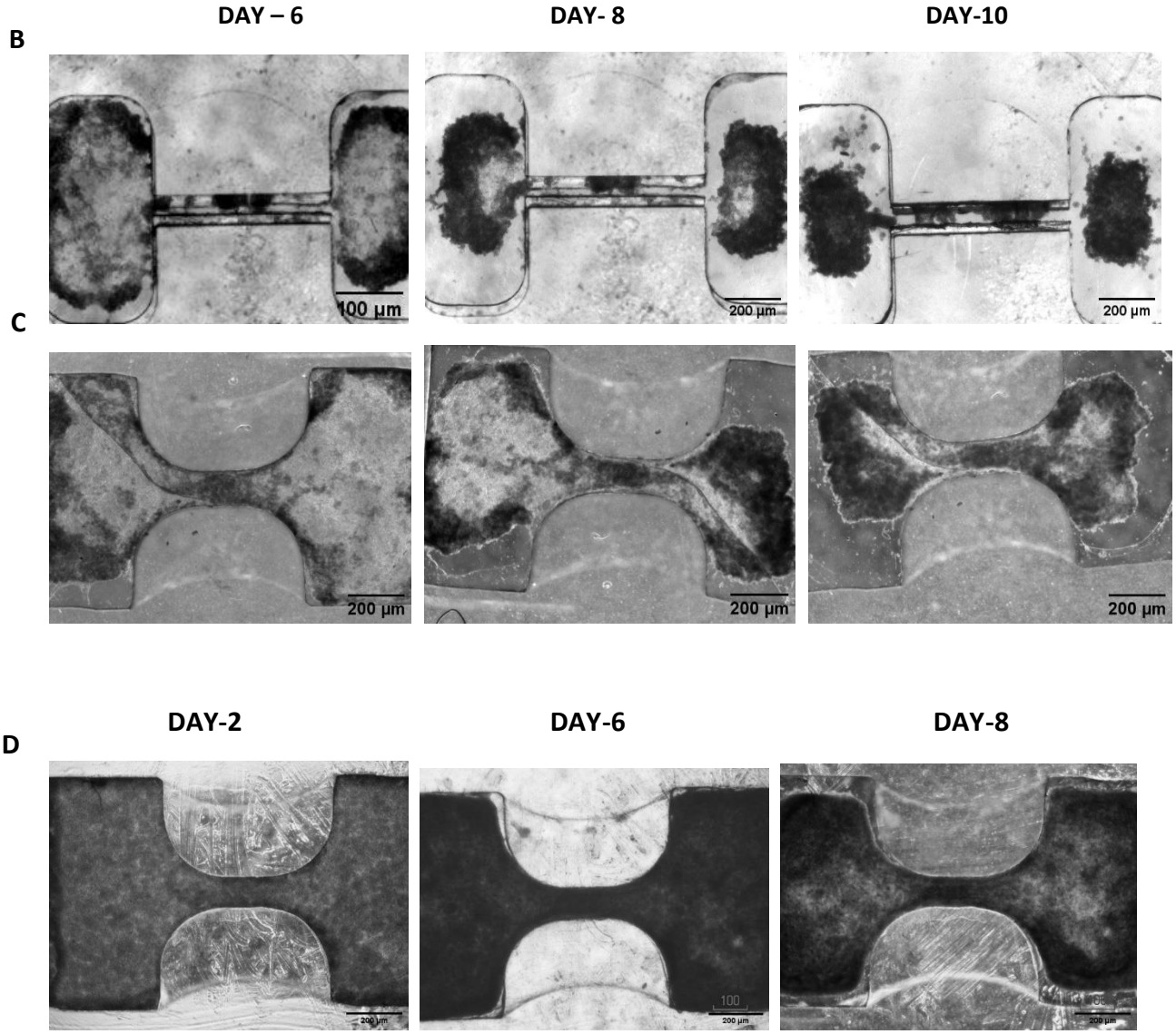

Figure 4: Overview of the PMMA and PDMS shape formation. *(A) Overview of the cell organization process over time in both PMMA and PDMS shapes. (B, C) Comparision of the arrhythmic shape formation by cardiomyocytes in PMMA (B) and PDMS (C). (D) Optimized PDMS chip with fixed position in the 12-well plate using high vaccum grease.*

PDMS	PMMA
The shapes looked complete and are connected through the channel without any breakage of cells.	The shapes didn't look filled, and the cells are scattered over the shape.
Xanthan gum is difficult to remove from the PDMS shapes as it is in the reservoir and needs couple of washing steps on the day of staining to completely remove it.	In PMMA shapes, xanthan gum is easy to take off from the surface of cells with regular refreshment of CM medium as the shapes are extruded in the plate.
The calcium imaging and confocal imaging might be a little challenging, as the PDMS shapes are not fixed to the plates.	In PMMA the shapes are in a fixed position on the plate so the shapes can be directly imaged.
The PDMS shapes cannot be reused and stock of PDMS shapes should be made from time to time which is quite laborious.	The PMMA plates can be reused, and PCR adhesive tapes are used to seal the bottom of the plate which is cheap.

Table 1: Overview of the differences between the PDMS and PMMA shapes

3.2.Hinderance occurred with staining

To test if the calcium staining solution is efficient, hiPSC-derived cardiomyocytes were seeded as monolayers and calcium staining were performed in monolayers and PDMS shapes. Once the cells commenced beating, calcium staining was conducted on both the monolayers and the PDMS shapes to compare Ca2+ transient levels in cardiomyocytes. For this, 5 PDMS shapes and 3 monolayer shapes were generated and maintained through medium refreshments until the 10^{th} day.

Figure 5 depicts fluorescent signals observed in the cardiomyocyte monolayers, affirming that the staining solution is not the issue. Instead, the inadequate staining of the PDMS shapes is attributed to the presence of the xanthan gum layer.

A

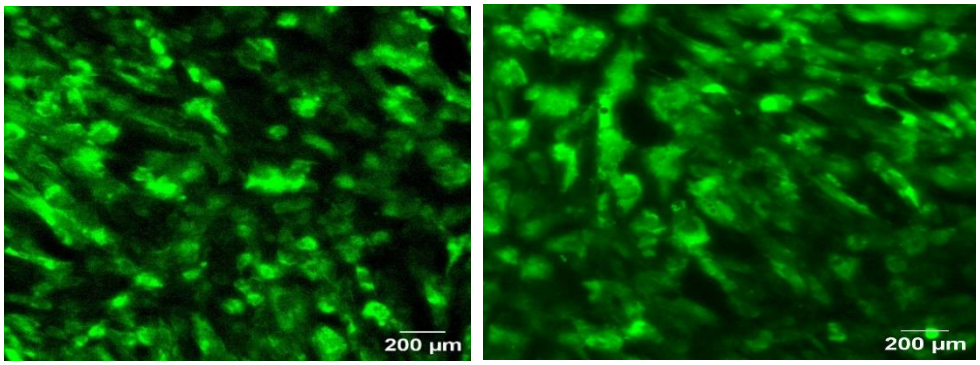

Figure 5: Fluorescent signals to monitor calcium transients. A) monolayers (n=5).

3.3. Xanthan gum affects the calcium staining

The optimization of the culture conditions and PDMS shapes was imperative for the successful cultivation of cardiomyocytes, ensuring the maintenance of a robust dumbbell structure and the initiation of rhythmic beating. The experiment involving monolayers on 96-well plate and PDMS shapes revealed that xanthan gum contributed to inadequate staining. When 2% xanthan gum mixture was employed to overlay the cell monolayer and prevent tissue compaction, no fluorescent signals or calcium sparks were detected, even though the shapes exhibited proper beating under a bright-field microscope. This might be because of the presence of a thin layer of Xanthan gum upon the cells which did not allow the cells to contract enough as seen in the Figure 6A. The high concentration of the 2% xanthan gum solution made it difficult to thoroughly wash off, suspected to be inhibiting adequate cell contraction even around Day-9. These staining and contraction issues likely resulted from the xanthan gum layer, impeding dye absorption, and causing unsuccessful staining. After conducting cell culturing experiments with 2% and 1.5% xanthan gum solutions, 1.5% Xanthan Gum was selected for future experiments (Figure 6B). This refinement in methodology proved to be pivotal, making progress in overcoming challenges encountered during the initial stages of this study.

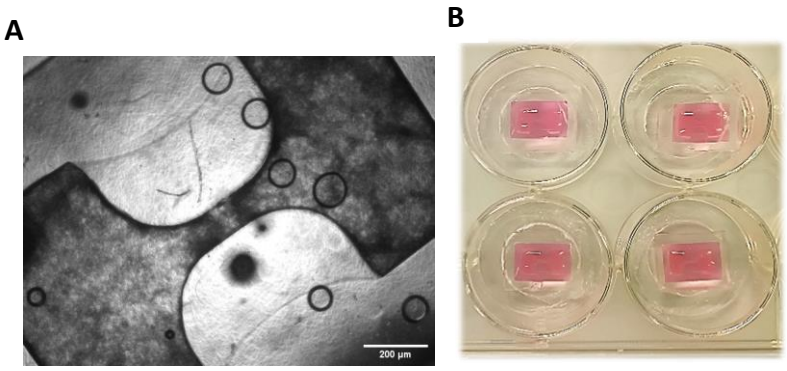

Figure 6: Arrhythmic shapes with Xanthan gum on top*. (A) Cardiac tissue on PDMS shape on day 8. (B) Top view representation of X.G on the PDMS shape.*

3.4.Effect of Epinephrine and Amiodarone on cardiac tissue

Following the successful optimization of the PDMS chip, cardiac tissues underwent testing with the anti-arrhythmic drug Amiodarone to assess the drug's impact on the irregular beating rhythm induced by adrenergic stimulant epinephrine. Among the experiments conducted, three displayed a similar pattern of the effect of the drug epinephrine and Amiodarone, and the most representative one is used for the data analysis and the results are presented in Figure 7. To access the activation time of the signal in the tissue and to analyze the arrhythmia's signal re-entry phenomenon, optical mapping with BV workbench software was employed. Within this software, we can generate action potential duration and activation time maps, providing insights into signal origins and endpoints. This feature is instrumental in estimating whether there is a re-excited signal, discernible through changes in the color palette. To verify its compatibility with our data, an optical mapping analysis was conducted on a shape demonstrating robust signal propagation, as illustrated in Figure 7A. The color variation in Figure 7A indicates that signal propagation originates from the bottom right corner, travels through the isthmus, and reaches the left side of the shape within a 3-second timeframe. Although time constraints limited extensive data generation, a successful optical mapping analysis on a shape with good signal propagation confirmed the

software's viability with the data from PDMS shapes. This allowed for moving forward with analyzing arrhythmia and studying how signal propagation changes with the administration of anti-arrhythmic drugs.

Upon treatment, with 0.1 µM Epinephrine, an increased number of peaks could be detected, indicating a higher frequency rate (Hz). Upon administration of 0.1 µM Amiodarone, there was minimal difference in frequency rate because of the short duration of the video (Figure 7B). To assess the effect of Amiodarone, a closer analysis of the intensity peaks shows that the refractory period increases with increasing concentrations of Amiodarone. A concentration dependent increase in the refractory period is observed (Figure 7C). Figure 7D and 7E shows the averaged refractory period (ms) and averaged frequency rate (Hz) in the obtained Ca2+ intensity peaks of the cardiac tissues respectively.

Subsequently, in the optical mapping phase, results from the same experiment with spontaneous beating, 0.1 µM Epinephrine and 0.1 µM Amiodarone were utilized to generate activation time maps, as depicted in Figure 7F, 7G and 7H respectively. Between the baseline and Epinephrine, there is not much difference in the activation time of the signal as shown in Figure 7F and 7G. However, the introduction of Amiodarone increased the activation time duration from 160 ms to 300 ms, indicating a slowdown in duration of activation time (Figure 7H). According to literature, the administration of class IC anti-arrhythmic drug Flecainide and class III anti-arrhythmic drug Dofetilide are reported to extend the cycle length duration and action potential duration in the activation maps, leading to a deceleration of conduction velocity in rotor cardiac tissue models [28].

Combined with our intensity graph results, we can partially conclude that Epinephrine increases the frequency rate (Hz), but it does not have a significant effect on the action potential duration and refractory period. It was also observed that activation time and refractory period were upregulated when Amiodarone was administrated. Our results were in accordance with results from literature depicting that Epinephrine increases the heart rate (frequency rate), but the effect on the duration of action potential and refractory period were not significant [29], [30], [31]. Recent investigations show that Amiodarone inhibits potassium currents responsible for repolarization, leading to an increase in the duration of action potential and refractory period of cardiac cells which is also observed in our results (7C) [32]. However, due to the novelty of this data analysis and time constraints, the specific data values required to calculate conduction velocity were not generated and in addition, time constraints limited extensive data generation using this optical mapping software. Future experiments aligned with optical mapping could enhance the comprehensive study of anti-arrhythmic drug effects on events resembling arrhythmia.

A

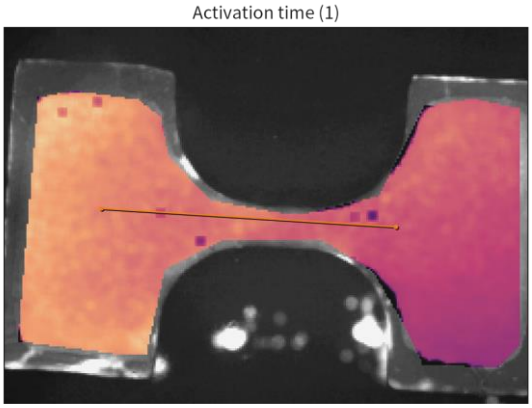

B

Spontaneous beating

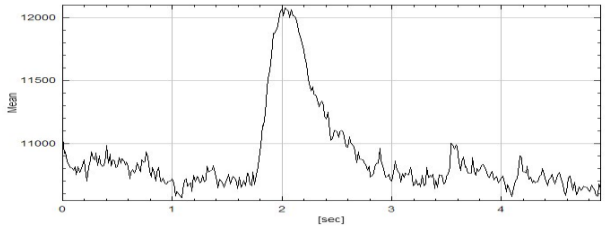

0.1 µm Epinephrine

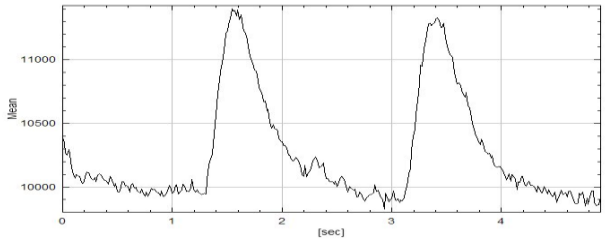

0.1 µm Amiodarone

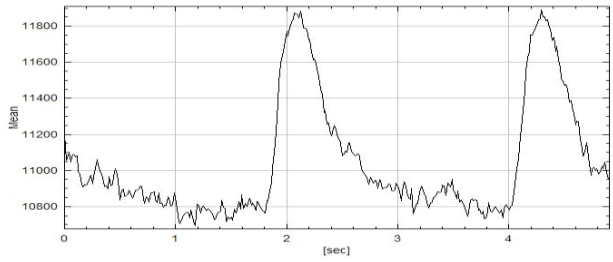

C

0.1 µm Amiodarone

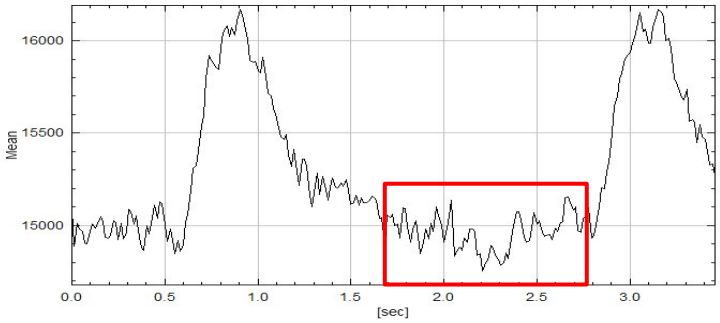

1000 ms

1 µm Amiodarone

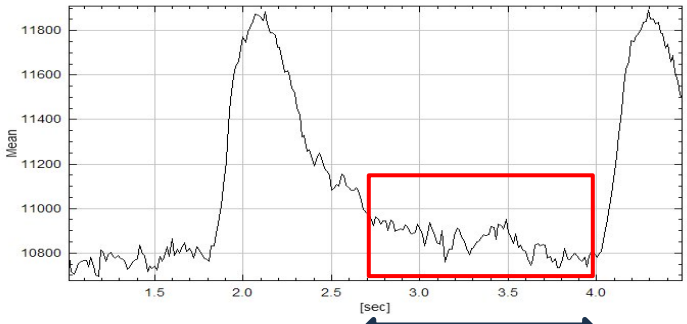

1300 ms

10 µm Amiodarone

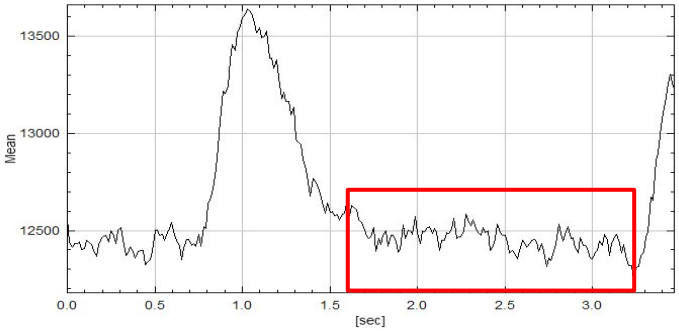

1500 ms

D

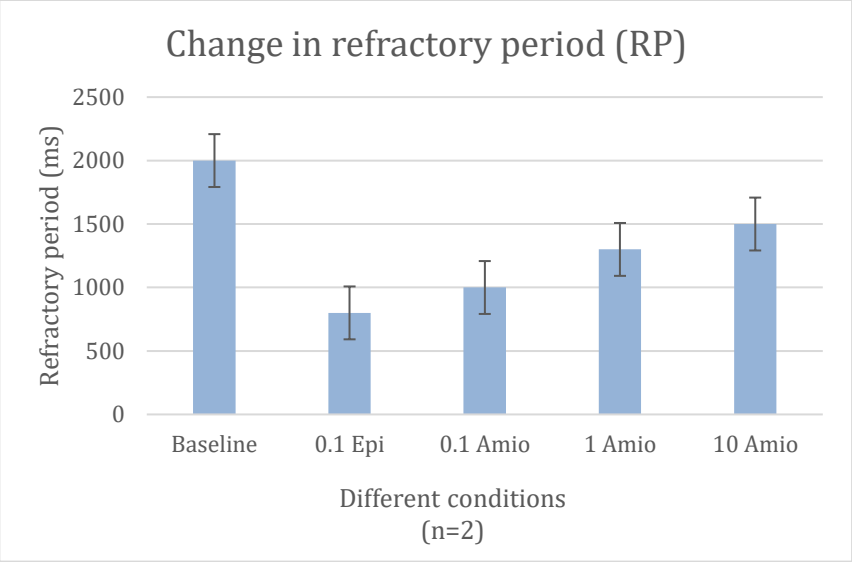
Change in refractory period (RP)
Refractory period (ms)
2500
2000
1500
1000
500
0
Baseline
0.1 Epi
0.1 Amio
1 Amio
10 Amio
Different conditions
(n=2)

E

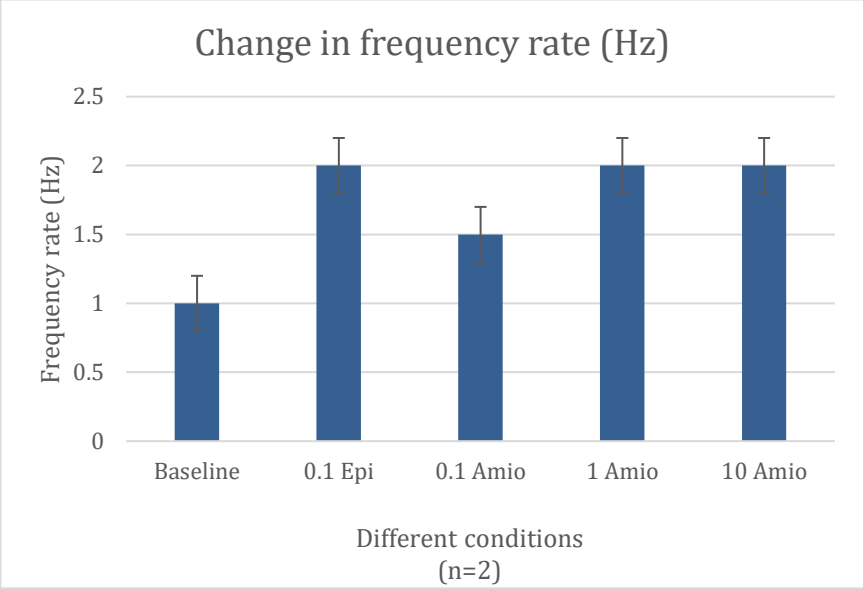
Change in frequency rate (Hz)
Frequency rate (Hz)
2.5
2
1.5
1
0.5
0
Baseline
0.1 Epi
0.1 Amio
1 Amio
10 Amio
Different conditions
(n=2)

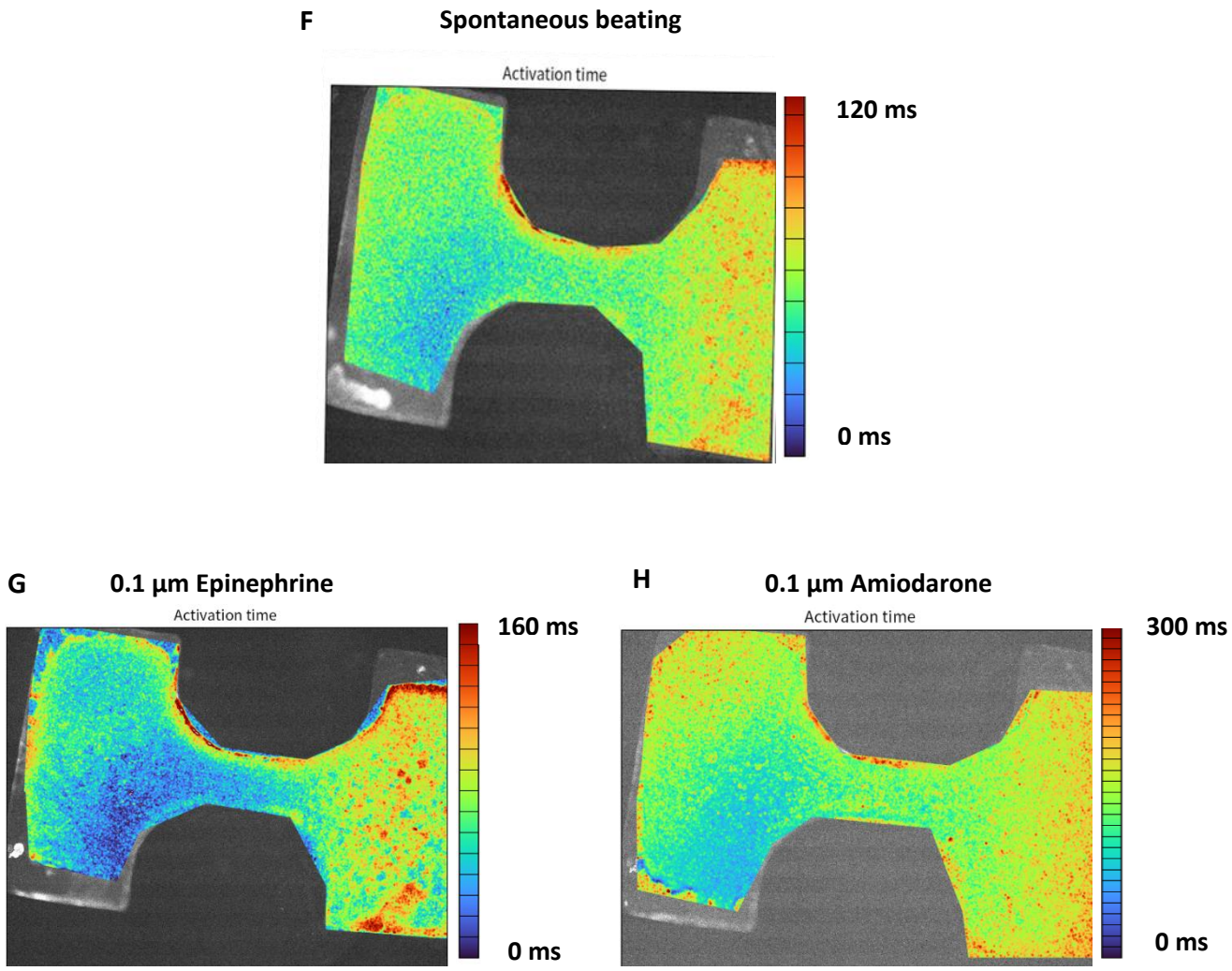

Figure 7: Assessment of effect of epinephrine and amiodarone in cardiac tissue with Ca2+ intensity peaks and activation time maps. *(A) Cardiac tissue in PDMS shape with no treatment which exhibits a signal propagation at the earlier stage of the study (B) Difference in the Ca2+ intensity peaks of cardiac tissue with spontaneous beating, 0.1 µM epinephrine and 0.1 µM amiodarone administration (C) Difference in the refractory period of cardiac tissue with different concentrations of amiodarone (D) Averaged refractory period(ms) in the intensity peaks of cardiac tissues (n=2) at baseline, 0.1 µM epinephrine and Amiodarone (0.1 µM, 1 µM and 10 µM). (E) Averaged frequency rate (Hz) in the intensity peaks of cardiac tissues (n=2) at baseline, 0.1 µM epinephrine and Amiodarone (0.1 µM, 1 µM and 10 µM). Error bars represent standard error of mean. (F) Activation time map of spontaneous beating in cardiac tissue with a timeline for duration for Ca2+ signal propagation (G) Activation time map of 0.1 µM epinephrine in cardiac tissue with a timeline for duration for Ca2+ signal propagation (H) Activation time map of 0.1 µM amiodarone in cardiac tissue with a timeline for duration for Ca2+ signal propagation.*

3.5. Electrical pacing and drug testing

Challenges persisted with PDMS shapes during imaging, as they tended to float in the wells plate when CM medium was added. Looking ahead, the next step is focused pacing of the cells with electrodes to assess propagation of the electrical signal. In addition, this could potentially generate a faster rhythm, allowing the evaluation of anti-arrhythmic drug effects on induced arrhythmia. Incorporating electrodes into the PDMS shapes required a fixed position for proper contact. An engineered cap was considered to secure the electrodes without disturbance as shown in the Figure 8A.

After achieving this fixed cardiac model for optimal pacing, the next step was to deliberately induce arrhythmia in the shapes through electrical pacing, aiming to comprehend the re-entry phenomena and facilitate the testing of anti-arrhythmic drugs. Initially, arrhythmia was successfully induced using the adrenergic stimulant epinephrine, prompting us to replicate the induced arrhythmia using electrical pacing. To achieve this, cells must adhere to electrical pacing, conducting signals across the shapes. To validate this theory, cells were paced at various voltages and increasing frequencies, to optimize the pacing conditions for arrhythmia induction as the signal traversed from the larger area through the narrowed channel. Pacing experiments were conducted at 10 V from frequencies 1-5 Hz, and at 20 V from frequencies 1-5 Hz with a 10 Am current. Regrettably, the pacing attempts yielded unsuccessful results as the cells failed to respond to the electrical signals. Subsequently, the anti-arrhythmic drug Amiodarone was examined at concentrations of 0.1 µM and 1 µM to assess its impact on the paced tissues. Cell imaging conducted for a duration of 15 seconds under four conditions (Figure 8B, 8C,8D and 8E). Even though, the cells did not follow the electrical pacing, the cardiac cells revealed a decrease in Ca2+ intensity peaks following Amiodarone administration. However, this outcome does not provide conclusive evidence regarding the cells' responsiveness to electrical pacing.

A

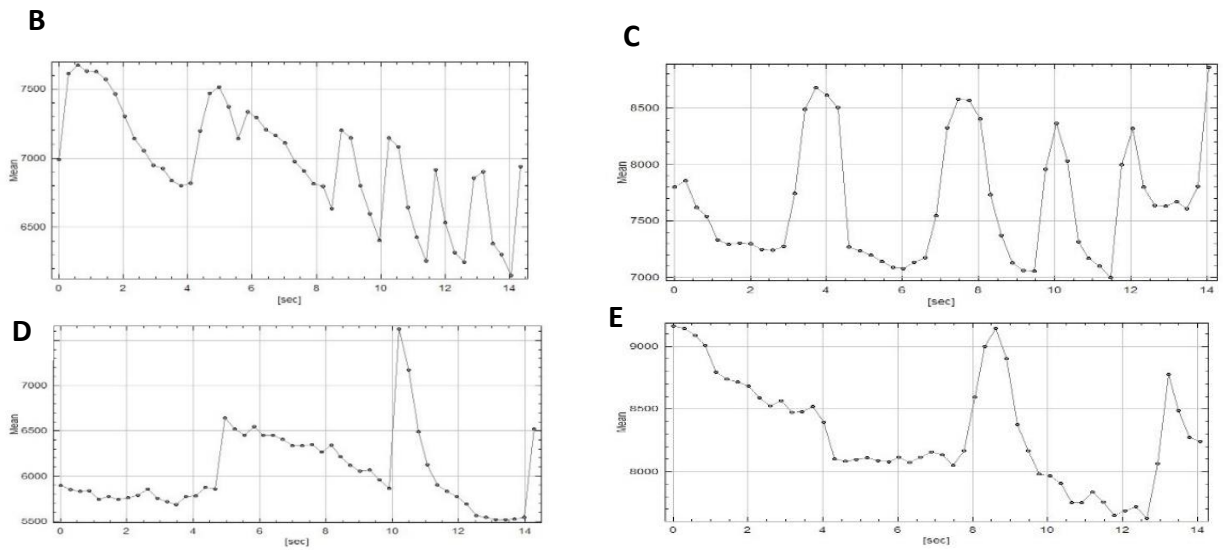

Figure 8: Intensity graphs of cardiac tissues*. (A) setup of the electrical pacing using the customer holder for electrodes**. (B) Baseline measurement of the PDMS cardiac tissue. (C) Cardiac tissue when paced at 20V, 5Hz. (D) Cardiac tissue after administration of 0.1 µM of Amiodarone. (E) Cardiac tissue after administration of 1 µM concentration of Amiodarone.*

Several attempts, totaling five experiments, were made to electrically stimulate cells using electrodes, but the outcomes were inconsistent and one of the results in presented in the Appendix Figure 9. Close contact of the electrodes with the shape led to tissue destruction. Consequently, the electrodes were positioned in the surrounding area of the shape within the PDMS reservoir, disrupting the electrical signal. This disruption occurred because the outer layer of the shape was in contact with the medium, causing the signal to disperse and travel from both sides of the shape. Consequently, when pacing was supposed to be initiated from one side, the signal initiated from both sides due to medium contact, reaching its conclusion at the isthmus tunnel. This scenario posed a challenge in sustaining pacing to induce arrhythmia. The experiment suggests that cells respond to electrical signals, but whether they generate an arrhythmic event on the opposite side when electrically paced from one side remains unclear. While alternative methods using graphite/PDMS composites existed, direct application on the glass slide posed challenges in connecting to external electricity conducting wires and lacked evidence of biocompatibility in cell culture, leading to the exclusion of this option.

Microelectrode Arrays (MEAs) are surface systems featuring closely spaced multichannel electrodes designed for cell culture. The number, size, and structure of these electrodes can be customized to suit the specific cell type under investigation. MEAs have the capability to record both the field potential and electrophysiological properties of the cell monolayer [34],[35],[36]. From recent studies, it is known that MEAs can be customized to determine the action potential of hiPSC- derived CMs and their biomechanical properties [37], [38], [39]. The isthmus structure within the PDMS chip is a crucial factor in arrhythmia induction in this study. Existing MEAs proved inadequate for comprehending arrhythmic conditions. Literature suggests that crafting a chip with high-density electrodes could revolutionize drug testing for arrhythmia and other cardiovascular diseases, particularly with the development of the CardioMEA data analysis platform. This advancement aims to enhance precision and accuracy in electrophysiology measures, particularly for analyzing MEA data [39].

During the initial data analysis, several challenges were encountered in optical map creation, including issues with data format, frames per second (fps), exposure time, and the time frame of the movie. It was determined that the fps should be set to at least 50 fps, a requirement not initially met. Through these experiments, it becomes evident that calcium imaging with staining poses challenges, and the use of Fluo-8 AM can make the procedure costly. Assessing action potential conduction velocity solely through bright field data would offer more advantages. The collaboration with Antti Ahola, a researcher from Tampere University, Finland, has enabled the realization of this possibility. The researcher introduced in-house developed MATLAB based data analysis software called CellVisus. This analysis aimed to detect electrophysiological properties and electrical signal propagation without relying on fluorescence. This introduces a novel spatiotemporal segmentation method, showcasing its application on a hiPSC-CM monolayer [33]. The methodologies outlined serve as a foundation for investigating the relationships between cellular structure and contractile function. The software utilizes bright field microscopy to capture videos of cardiac tissue beatings. This approach has the potential to yield the desired results without the need for staining cells with calcium dye and imaging Ca2+ signals. Limited time availability resulted in a restricted generation of results. The result dataset comprises an image depicting the magnitude of contraction in pixels, an image illustrating the propagation of contraction through the shape, and a graph plotting the contraction and relaxation velocities against the video frames. The results are presented in Appendix Figure 10. As previously discussed, calcium staining posed a challenge due to the thin layer of Xanthan gum covering the cells. Segmentation based on Power Spectral Density (PSD) offers a method of segmentation focused on cell function. The primary goal was to identify areas exhibiting movement related to contraction. This segmentation not only facilitates the detection of contraction-related movement but also enables the tool to offer additional spatial information. This includes the quantification of contraction propagation within the given context. Exploring different approaches using segmentation for data analysis for cardiac tissues could be a promising future option, as it eliminates the need for staining.

4. Conclusion

This study represents the initial steps in developing a heart-on-chip model to assess the risk of cardiac arrhythmias. The research highlights the model's effectiveness in studying arrhythmias within a human heart-on-chip context. The optimization of culture conditions and PDMS chips has facilitated improved calcium imaging. The specifically designed PDMS arrhythmia shapes have shown promise for pro-arrhythmic drug testing. The study reveals concordant effects of epinephrine and amiodarone, aligning with existing literature and opening the door for testing other adrenergic stimulants and anti-arrhythmic drugs. Furthermore, the findings suggest that the current electrical pacing technique is ineffective in stimulating cardiac tissue in PDMS shapes, advocating for the exploration of more refined pacing techniques in future investigations. Looking forward, there is potential to advance this heart-on-chip model into a versatile, multidisciplinary platform for a comprehensive assessment of the risk of cardiac arrhythmias.

5. Appendix A – Supplementary Figures

In Figure 9, Ca2+ intensity peaks are depicted following electrical pacing of cardiac tissues at 20V with various frequencies. This experiment aimed to assess if the cardiac tissues follow the electrical signal when paced from one side of the shape. Regrettably, the results remain inconclusive.

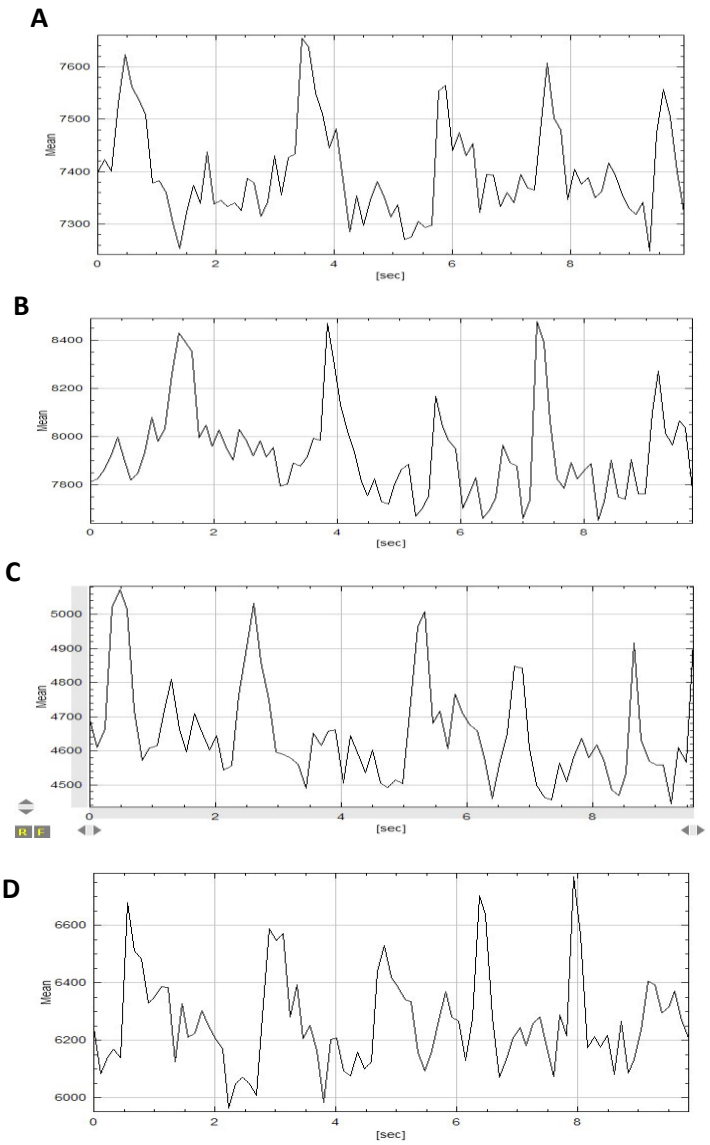

Figure 9: Ca2+ intensity peaks of the cardiac tissue in PDMS shape*. (A) Intensity graph of the tissue when paced at 20V, 10 A current,1 Hz (A), 2 Hz (B), 3 Hz (C), and 4 Hz (D).*

Figure 10 illustrates the outcomes obtained through the MATLAB-based data analysis software CellVisus. The analysis involved the examination of bright-field microscopy videos capturing the beating cardiac tissue, with the resulting data presented below. Figure 10B visually represents the magnitude of contraction in pixels, effectively portraying its spread. Enhanced light transmission could provide more detailed insights into the propagation process. Additionally, Figure 10C exhibited the anticipated propagation results, showcasing a well-defined spread of contraction originating from the isthmus. The illustration reveals the organic spread, with the darkest red spots representing artifacts. In Figure 10D, the x-axis represents the video frame, while the y-axis depicts the mean motion in pixels between frames. The upward transient signifies contraction velocity, and the downward transient represents relaxation velocity. The peak of the transient indicates the highest velocity, corresponding to the frame with the fastest motion. The videos provide a measure of matter displacement rather than force.

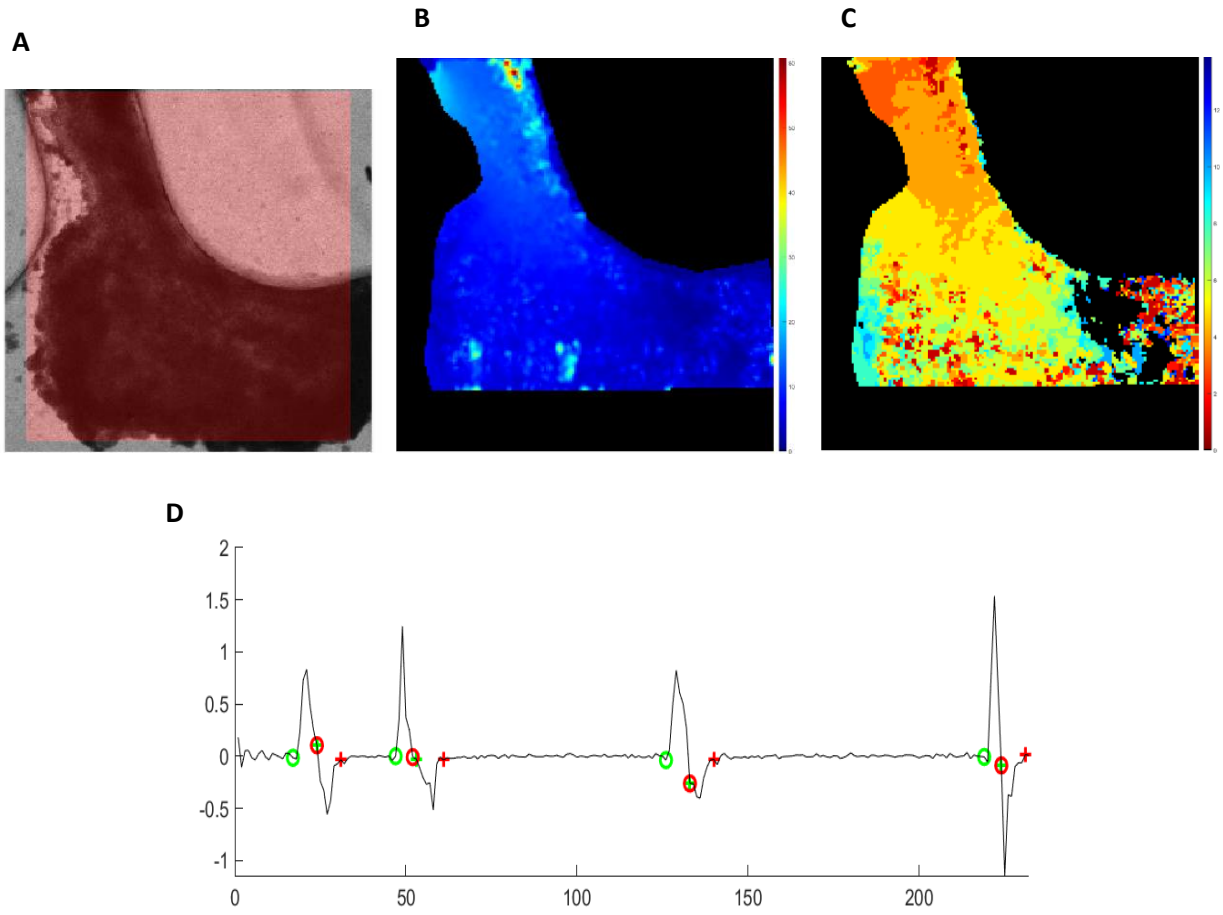

Figure 10: Overall results from CellVisus Data Analysis software. *(A) The input data of the cardiac tissue for the data analysis (B) Image of the magnitude of contraction in pixels. (C) Image of the propagation of contraction through the shape. (D) Graph of the contraction velocity and relaxation velocity plotted against the video frame.*

6. References

[1] A. D'Alessandro, I. Boeckelmann, M. Hammwhöner, and A. Goette, "Nicotine, cigarette smoking and cardiac arrhythmia: An overview," *European Journal of Preventive Cardiology*, vol. 19, no. 3. pp. 297–305, Jun. 2012. doi: 10.1177/1741826711411738.

[2] G. A. Roth *et al.*, "Global Burden of Cardiovascular Diseases and Risk Factors, 1990-2019: Update From the GBD 2019 Study," *Journal of the American College of Cardiology*, vol. 76, no. 25. Elsevier Inc., pp. 2982–3021, Dec. 22, 2020. doi: 10.1016/j.jacc.2020.11.010.

[3] M. Ezeani, "Aberrant cardiac metabolism leads to cardiac arrhythmia," 2020.

[4] E. G. Nabel, "Cardiovascular Disease," *New England Journal of Medicine*, vol. 349, no. 1, pp. 60–72, Jul. 2003, doi: 10.1056/NEJMra035098.

[5] "Health disease- Arrhythmia." Accessed: Aug. 07, 2023. [Online]. Available: https://my.clevelandclinic.org/health/diseases/16749-arrhythmia

[6] J. Heijman, H. Sutanto, H. J. G. M. Crijns, S. Nattel, and N. A. Trayanova, "Computational models of atrial fibrillation: Achievements, challenges, and perspectives for improving clinical care," *Cardiovascular Research*, vol. 117, no. 7. Oxford University Press, pp. 1682–1699, Jun. 15, 2021. doi: 10.1093/cvr/cvab138.

[7] P. R. R. van Gorp, S. A. Trines, D. A. Pijnappels, and A. A. F. de Vries, "Multicellular In vitro Models of Cardiac Arrhythmias: Focus on Atrial Fibrillation," *Front Cardiovasc Med*, vol. 7, 2020, doi: 10.3389/fcvm.2020.00043.

[8] M. J. Prust, W. G. Stevenson, G. R. Strichartz, and L. S. Lilly, "Mechanisms of cardiac arrhythmias," in *Pathophysiology of Heart Disease: A Collaborative Project of Medical Students and Faculty*, Wolters Kluwer Health, 2015, pp. 268–286. doi: 10.1016/j.rec.2011.09.020.

[9] "Arrhythmia conditions." Accessed: Aug. 07, 2023. [Online]. Available: https://www.bhf.org.uk/informationsupport/conditions/arrhythmias

[10] "Health disease- Arrhythmia." Accessed: Aug. 07, 2023. [Online]. Available: https://my.clevelandclinic.org/health/diseases/16749-arrhythmia

[11] K. Kocadal, "İlaca Bağlı Kardiyovasküler Risk: Geri Çekilen İlaçların Retrospektif Değerlendirilmesi," *North Clin Istanb*, 2018, doi: 10.14744/nci.2018.44977.

[12] O. J. Wouters, M. McKee, and J. Luyten, "Estimated Research and Development Investment Needed to Bring a New Medicine to Market, 2009-2018," *JAMA*, vol. 323, no. 9, pp. 844–853, Mar. 2020, doi: 10.1001/jama.2020.1166.

[13] "Healthy heart." Accessed: Aug. 07, 2023. [Online]. Available: https://www.heartandstroke.ca/heart-disease/what-is-heart-disease/how-a-healthy-heart-works

[14] Myrna LaFleur Brooks, "Arrhythmia vs Dysrhythmia." Accessed: Jan. 13, 2024. [Online]. Available: https://medicalterminologyblog.com/arrhythmia-dysrhythmia/

[15] M. B. Katan and E. Schouten, “Caffeine and arrhythmia 1-3,” 2005. [Online]. Available: www.medscape.com/viewarticle/491110

[16] M. J. Prust, W. G. Stevenson, G. R. Strichartz, and L. S. Lilly, “Mechanisms of cardiac arrhythmias,” in *Pathophysiology of Heart Disease: A Collaborative Project of Medical Students and Faculty*, Wolters Kluwer Health, 2015, pp. 268–286. doi: 10.1016/j.rec.2011.09.020.

[17] J. Criscione *et al.*, “Heart-on-a-Chip Platforms and Biosensor Integration for Disease Modeling and Phenotypic Drug Screening,” 2022.

[18] D. S. Auerbach, K. R. Grzęda, P. B. Furspan, P. Y. Sato, S. Mironov, and J. Jalife, “Structural heterogeneity promotes triggered activity, reflection and arrhythmogenesis in cardiomyocyte monolayers,” *Journal of Physiology*, vol. 589, no. 9, pp. 2363–2381, May 2011, doi: 10.1113/jphysiol.2010.200576.

[19] L. Kimlin, J. Kassis, and V. Virador, “3D in vitro tissue models and their potential for drug screening,” *Expert Opin Drug Discov*, vol. 8, no. 12, pp. 1455–1466, Dec. 2013, doi: 10.1517/17460441.2013.852181.

[20] A. J. Ryan, C. M. Brougham, C. D. Garciarena, S. W. Kerrigan, and F. J. O’Brien, “Towards 3D in vitro models for the study of cardiovascular tissues and disease,” *Drug Discov Today*, vol. 21, no. 9, pp. 1437–1445, 2016, doi: https://doi.org/10.1016/j.drudis.2016.04.014.

[21] S. Caddeo, M. Boffito, and S. Sartori, “Tissue Engineering Approaches in the Design of Healthy and Pathological In Vitro Tissue Models,” *Front Bioeng Biotechnol*, vol. 5, 2017, doi: 10.3389/fbioe.2017.00040.

[22] O. Mourad, R. Yee, M. Li, and S. S. Nunes, “Modeling Heart Diseases on a Chip: Advantages and Future Opportunities.,” *Circ Res*, vol. 132, no. 4, pp. 483–497, Feb. 2023, doi: 10.1161/CIRCRESAHA.122.321670.

[23] I. Jorba, D. Mostert, L. H. L. Hermans, A. van der Pol, N. A. Kurniawan, and C. V. C. Bouten, “In Vitro Methods to Model Cardiac Mechanobiology in Health and Disease,” *Tissue Eng Part C Methods*, vol. 27, no. 3, pp. 139–151, 2021, doi: 10.1089/ten.tec.2020.0342.

[24] N. Harlaar *et al.*, “Conditional immortalization of human atrial myocytes for the generation of in vitro models of atrial fibrillation,” *Nat Biomed Eng*, vol. 6, no. 4, pp. 389–402, 2022, doi: 10.1038/s41551-021-00827-5.

[25] E. J. Ciaccio, J. Coromilas, A. L. Wit, N. S. Peters, and H. Garan, “Source-Sink Mismatch Causing Functional Conduction Block in Re-Entrant Ventricular Tachycardia,” 2018.

[26] “tjp0516-0793”.

[27] Z. Zhao *et al.*, “Drug Testing in Human-Induced Pluripotent Stem Cell–Derived Cardiomyocytes From a Patient With Short QT Syndrome Type 1,” *Clin Pharmacol Ther*, vol. 106, no. 3, pp. 642–651, Sep. 2019, doi: 10.1002/cpt.1449.

[28] Z. Laksman *et al.*, “Modeling Atrial Fibrillation using Human Embryonic Stem Cell-Derived Atrial Tissue,” *Sci Rep*, vol. 7, no. 1, Dec. 2017, doi: 10.1038/s41598-017-05652-y.

[29] A. J. Fuenmayor A, L. Gómez R, and M. I. Solórzano, “Effects of epinephrine over P wave duration and ventricular repolarization in subjects without structural heart disease,” *Int J Cardiol*, vol. 204, pp. 142–146, Feb. 2016, doi: 10.1016/j.ijcard.2015.11.182.

[30] Y.-K. Ju and D. G. Allen, “How does β-adrenergic stimulation increase the heart rate? The role of intracellular Ca2+ release in amphibian pacemaker cells,” *J Physiol*, vol. 516, no. 3, pp. 793–804, May 1999, doi: https://doi.org/10.1111/j.1469-7793.1999.0793u.x.

[31] J. S. Cameron, G. H. Dersham, and J. Han, “Effects of epinephrine on the electrophysiologic properties of purkinje fibers surviving myocardial infarction,” *Am Heart J*, vol. 104, no. 3, pp. 551–560, 1982, doi: https://doi.org/10.1016/0002-8703(82)90226-5.

[32] “Drug bank/Amiodarone.” Accessed: Jan. 17, 2024. [Online]. Available: https://go.drugbank.com/drugs/DB01118

[33] A. Ahola and J. Hyttinen, “Spatiotemporal Quantification of In Vitro Cardiomyocyte Contraction Dynamics Using Video Microscopy-based Software Tool”, doi: 10.22489/CinC.2021.303.

[34] S. Kussauer, R. David, and H. Lemcke, “Microelectrode Arrays: A Valuable Tool to Analyze Stem Cell-Derived Cardiomyocytes,” in *Stem Cells: Latest Advances*, K. H. Haider, Ed., Cham: Springer International Publishing, 2021, pp. 1–20. doi: 10.1007/978-3-030-77052-5_1.

[35] C. M. Didier, A. Kundu, D. DeRoo, and S. Rajaraman, “Development of in vitro 2D and 3D microelectrode arrays and their role in advancing biomedical research,” *Journal of Micromechanics and Microengineering*, vol. 30, no. 10, p. 103001, 2020, doi: 10.1088/1361-6439/ab8e91.

[36] C. M. Kofron *et al.*, “A predictive in vitro risk assessment platform for pro-arrhythmic toxicity using human 3D cardiac microtissues,” *Sci Rep*, vol. 11, no. 1, p. 10228, 2021, doi: 10.1038/s41598-021-89478-9.

[37] X. Li, R. Zhang, B. Zhao, C. Lossin, and Z. Cao, “Cardiotoxicity screening: a review of rapid-throughput in vitro approaches,” *Arch Toxicol*, vol. 90, no. 8, pp. 1803–1816, 2016, doi: 10.1007/s00204-015-1651-1.

[38] “Development of a High-Density Microelectrode-Array-Based Platform for Studying Cardiac Arrhythmias and Drug Responses.” Accessed: Jan. 05, 2024. [Online]. Available: https://www.research-collection.ethz.ch/handle/20.500.11850/645862

[39] J. Lee, A. Hierlemann, F. Duru, H. Ulusan, and A. P. Buccino, “Development of a High-Density Microelectrode-Array-Based Platform for Studying Cardiac Arrhythmias and Drug Responses,” 2023. doi: 10.3929/ethz-b-000645862.